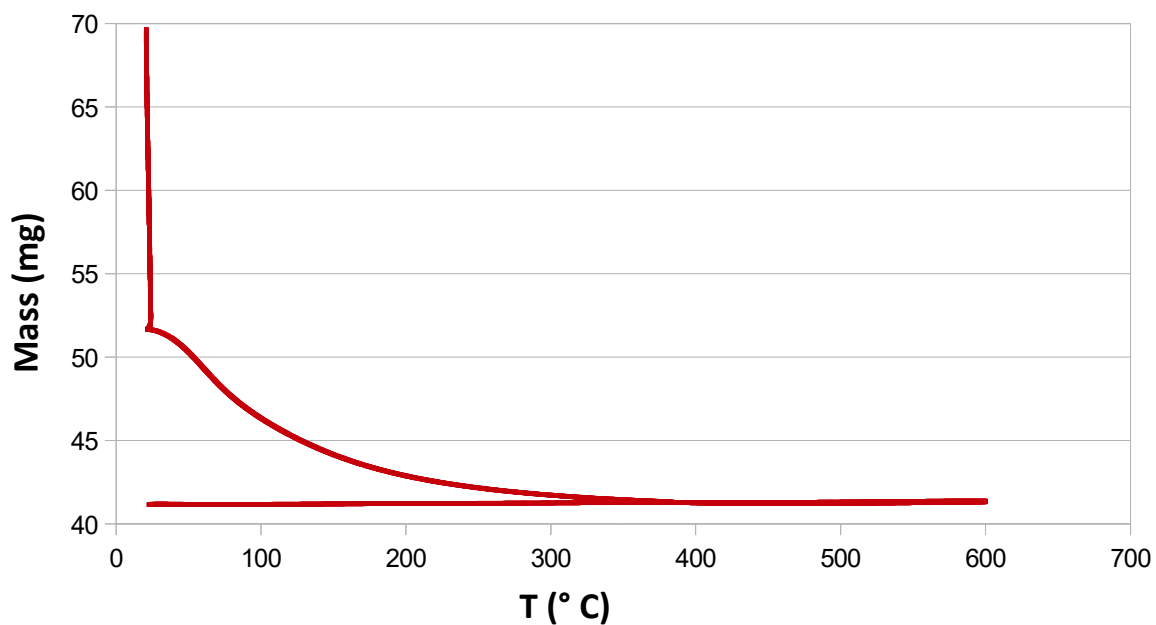


Supplementary data

**Single-step sintering of zirconia ceramics using hydroxide precursors and Spark Plasma**

**Sintering below 400°C**

C. Elissalde et al.



**Figure S1.** TGA of zirconium hydroxide under air (thermal ramp : 1°C/min)

Thermogravimetric analysis (TA Instrument Q50) of the raw powder shows an initial abrupt mass loss of 26 wt% at room temperature attributed to water desorption. Bounded hydroxyls are then released while increasing the temperature up to 200°C (16 wt% mass loss).

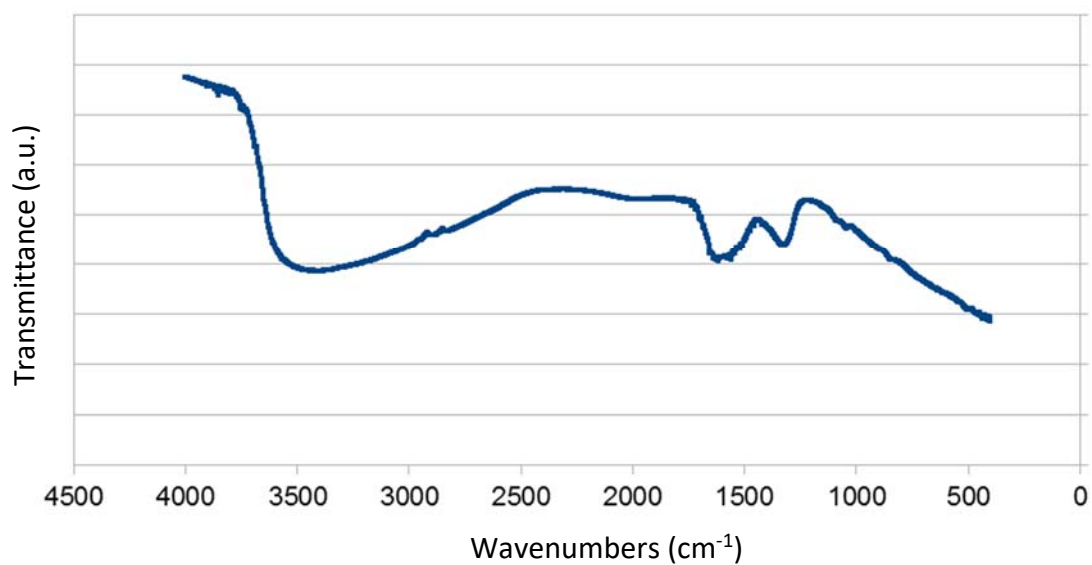


**Figure S2.** Infrared spectra of zirconium hydroxide

Infrared absorption spectrum (Brûler Equinox 55) confirms the presence of a large absorption band in the range 2500-3800 cm<sup>-1</sup> related to bounded OH and two bands in the range 1350-1650 cm<sup>-1</sup> assigned to surface absorbed hydroxyls.

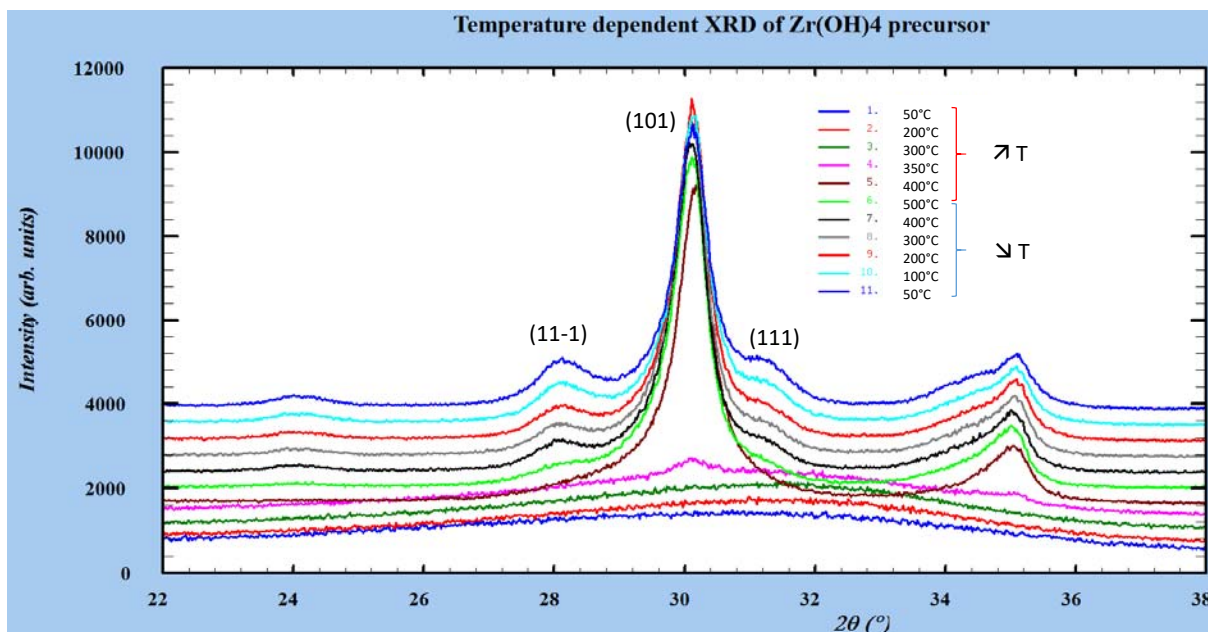


**Figure S3.** Powder X-ray Diffraction (PXRD - PANalytical X'Pert Pro diffractometer using  $\text{CuK}\alpha$  radiation ( $\lambda = 1.5406\text{\AA}$ )) at room temperature confirms the amorphous character of the raw powder. *In-situ* variable temperature PXRD (Philips X'Pert automatic diffractometer ( $\text{CuK}\alpha$  radiation) equipped with a variable-temperature Anton Paar HTK16 Pt stage) were performed from room temperature up to  $500^\circ\text{C}$  (heating rate  $5^\circ\text{C}/\text{min}$ ) recording patterns on heating and cooling every  $50^\circ\text{C}$ . Patterns recorded on heating and cooling every  $100^\circ\text{C}$  are shown.

The onset of crystallization of the amorphous phase into tetragonal phase occurs at  $300^\circ\text{C}$  with the intensity of the tetragonal (101) peak increasing abruptly in between  $350$  et  $400^\circ\text{C}$ . The monoclinic phase starts to crystallize above  $400^\circ\text{C}$ . The coexistence of the two polymorphs can be observed at  $500^\circ\text{C}$  (approximate fractions of 96% tetragonal / 4% monoclinic by PXRD analysis). The amount of monoclinic phase increases on re-cooling down to  $25^\circ\text{C}$ .

The main tetragonal peak (101) at  $\sim 30^\circ$  and the main monoclinic (11-1) and (111) peaks are reported on the graph.

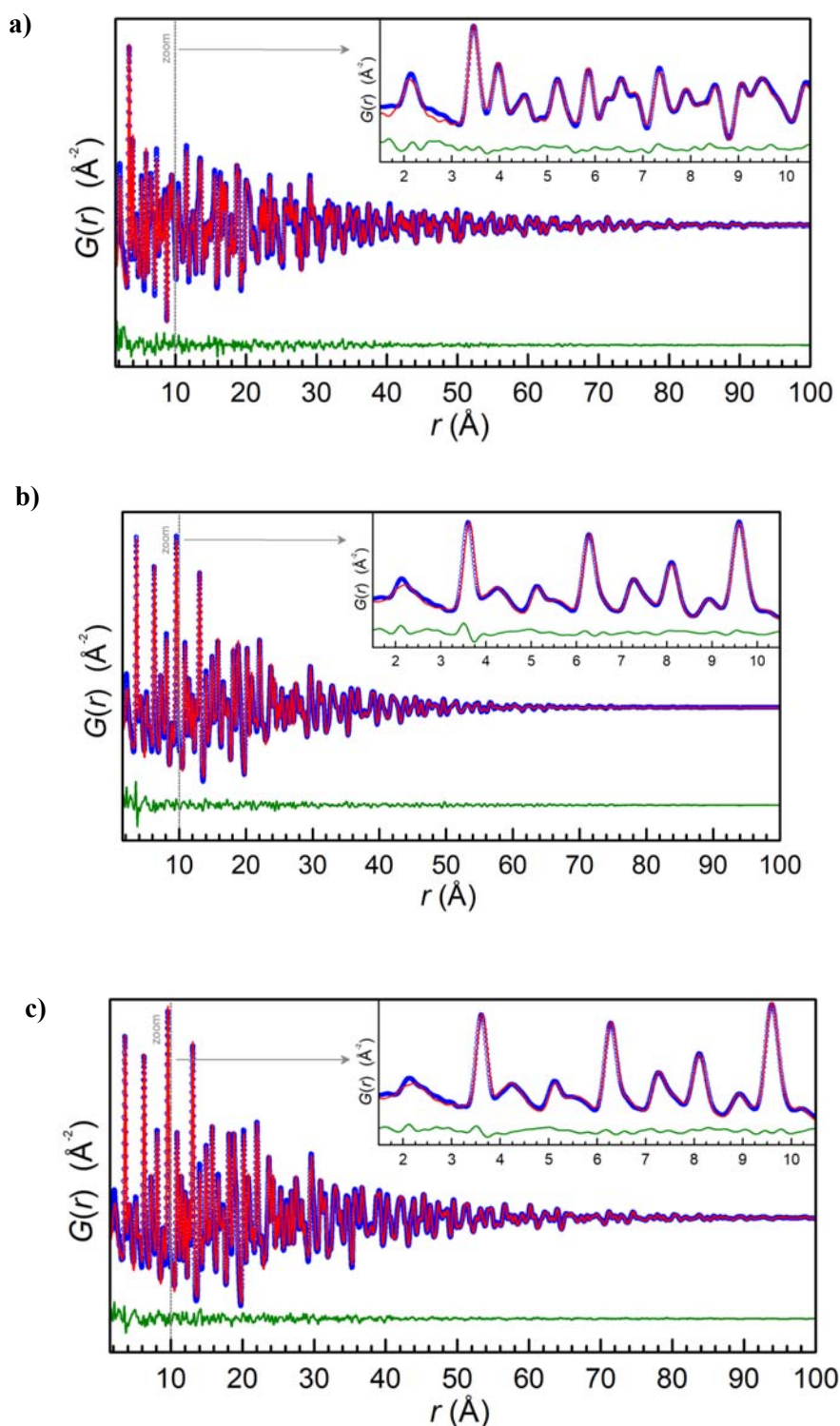


**Figure S4 (a-c)** : Fits of  $G(r)$  for references: a) the bulk monoclinic polymorph  $ZrO_2$  reference sample ( $Rwp = 13.5\%$ ). Lattice parameters for the refined structural model (space group  $P21/c$ ) are  $a = 5.155(1)$  Å,  $b = 5.206(1)$  Å,  $c = 5.322(2)$  Å, and monoclinic angle  $\beta = 99.209(2)^\circ$ . b) for the 'nano' tetragonal polymorph  $ZrO_2$  reference sample ( $Rwp = 10.1\%$ ). Lattice parameters for the refined structural model (space group  $P42/nmc$ ) are  $a = 3.615(1)$  Å,  $c = 5.170(2)$  Å. The fitted model includes a term for finite spherical crystallite size, which refines to a diameter of  $8.8(1)$  nm. c): Fit of  $G(r)$  for the bulk tetragonal polymorph  $ZrO_2$  reference sample ( $Rwp = 8.5\%$ ). Lattice parameters for the refined structural model (space group  $P42/nmc$ ) are  $a = 3.610(1)$  Å,  $c = 5.175(2)$  Å. Experimental data are plotted as blue circles, with the calculated fit and difference curves as red and green lines, respectively.